Available online at www.sciencedirect.com
ScienceDirect
Cement and Concrete Research 37 (2007) 303–309
Cement and Concrete Research

Two-dimensional correlation relaxometry studies of cement pastes performed using a new one-sided NMR magnet

Peter J. McDonald [a,*], Jonathan Mitchell [a], Mike Mulheron [b], Peter S. Aptaker [c], Jean-Pierre Korb [d], Luc Monteilhet [a,d]

[a] School of Electronics and Physical Sciences, University of Surrey, Guildford, Surrey, GU2 7XH, United Kingdom
[b] School of Engineering, University of Surrey, Guildford, Surrey, GU2 7XH, United Kingdom
[c] Laplacian Ltd., D5 Culham Science Centre, Culham Innovation Centre, Abingdon, Oxon, OX12 9LY, United Kingdom
[d] Laboratoire de Physique de la Matiére Condensée, UMR 7643 CNRS, Ecole Polytechnique, 91128 Palaiseu, France

Received 3 October 2005; accepted 17 January 2006

Abstract

We present preliminary results of the first NMR T_1–T_2 two-dimensional relaxation correlation experiments performed using a one-sided NMR system in cement based materials. Two-dimensional correlation relaxometry has itself only recently been demonstrated in cement paste where it proved to be a particularly sensitive probe of pore-water dynamics providing direct information on exchange of water between the gel and capillary pore networks. Further to this we have observed differences in the structural development of a selection of cement pastes throughout the early stages of hydration and verified the theoretical frequency dependence of the ratio T_1/T_2. When coupled with instrumentation developments in one-sided NMR magnets the way is opened to detailed, spatially resolved studies of the development of hydration and porosity in the surface layers (top 50 mm) of cementitious materials. A new magnet, suitable for such applications, is discussed.

Keywords: T_1–T_2 correlation; NMR relaxation analysis; Single-sided NMR

1. Introduction

In this paper we combine two recent developments in Nuclear Magnetic Resonance (NMR) methodology which offer future opportunity for detailed study of cement hydration and porosity development in the surface layers (0 to 50 mm) of built concrete structures. The first development is the measurement of two-dimensional correlation relaxometry in porous materials [1]. The second is a new one-sided NMR magnet that has been specifically designed and constructed for spatially resolved in situ characterisation of the built environment [2].

The NMR nuclear spin relaxation times T_1 and T_2 of magnetic species in liquids, usually ^{1}H (protons) in water, in porous media are sensitive probes of pore microstructure. In a two-dimensional correlation experiment, a relaxation time is "encoded" during the first period and a second relaxation time is measured in the second period. The two-dimensional Laplace inversion of the resultant data set shows the correlation of the relaxation time encoded in the first interval with that in the second. There is inherently more dynamic information in the two-dimensional experiment than in its one-dimensional counterpart. Almost any pair of T_1, T_2 or diffusion coefficient, D, can be correlated or self-correlated. Callaghan and Furo [3] have attempted to classify the possible variants and discuss their different merits. The methods are made possible with the recent demonstration by Venkataramanan et al. [4] of a robust algorithm for a two-dimensional inverse Laplace Transform. The solutions to the requisite equations for the coupled relaxation of two reservoirs [5,6] and the correlated diffusion [3] are known. Two-dimensional correlation experiments are rapidly being applied to oil-bearing rocks [7,8], to complex liquids [3] and to food [5]. We are the first group to apply them to a white cement paste [6]. Here we extend the study

* Corresponding author.
E-mail address: p.mcdonald@surrey.ac.uk (P.J. McDonald).

0008-8846/$ - see front matter © 2006 Elsevier Ltd. All rights reserved.
doi:10.1016/j.cemconres.2006.01.013

previously reported to follow the hydration of Ordinary Portland Cement (OPC) and to compare two different brands of white cement over 7 days. The results reveal different pore structure development in each of the samples. We also extend the work to much higher (400 MHz) and lower (2 MHz) NMR frequencies in order to more rigorously test our theoretical interpretation. These experiments clearly demonstrate the increase in information available compared to the one-dimensional relaxometry measurements hitherto used to study cement [9].

There is also growing interest in portable one-sided NMR systems for in situ applications addressing very large or immobile samples. Such systems include, for example, the NMR-MOUSE developed by Eidmann et al. [10] and down-bore-hole NMR logging tools developed by, for instance, Jackson et al. [11] and Kleinberg et al. [12]. Several authors have constructed magnets designed for the built environment. These target homogeneous field volumes displaced by a few centimetres from one side or end of the device [13–15]. In this work we move on to show that the two-dimensional correlation experiment can be performed on cement using a one-sided magnet, presenting a novel one-sided magnet design suitable for such work.

2. Relaxation analysis theory

Relaxometry relies on the fact that the nuclear spin relaxation times of nuclei (^{1}H NMR) in molecules of liquids such as water in the bulk are long (of the order of seconds) whereas the same relaxation times of nuclei in molecules temporarily adsorbed onto surfaces are much shorter (of the order of milliseconds). In porous media, where the surface (S) to volume (V) ratio is very large, the surface contribution to relaxation dominates. In the case that there is rapid averaging between "pore-bulk" and "pore-surface" molecules, a single, averaged relaxation time is observed [16]:

$$\frac{1}{T_{1,2}^{\text{observed}}} = \frac{1}{T_{1,2}^{\text{bulk}}} + \frac{\varepsilon S}{V}\frac{1}{T_{1,2}^{\text{surface}}} \tag{1}$$

where T_1 and T_2 are the spin-lattice and spin–spin relaxation times, respectively, and ε is the surface layer (assumed to be a mono-layer) thickness. Usually, $T_{1,2}^{\text{bulk}}$ is sufficiently large that the observed relaxation rate is directly proportional to S/V. The distribution of relaxation rates presented by a liquid filled porous medium is therefore a measure of the pore-size distribution. The method has been proven in a range of porous media including oil-bearing rocks [17–19]. It has also been used in cements [17,20,21].

Further progress towards the quantification of molecular dynamics in porous media has come from a model of $T_{1,2}^{\text{surface}}$ due to Godefroy et al. [22]. According to this model, temporarily adsorbed molecules (nuclear spins, I, here ^{1}H) undergo a two-dimensional random walk on the pore surface. As they repeatedly encounter paramagnetic species, S, the local dipolar fields are modulated causing relaxation. Two correlation times, the surface "hopping" time, τ_m, and the surface residency time, τ_s, are defined. The model leads to an expression for the frequency dependent ratio $T_{2,\text{surface}}/T_{1,\text{surface}}$, [6] viz:

$$\frac{T_{2,\text{surface}}(\omega_I)}{T_{1,\text{surface}}(\omega_I)} = 2 \times \left(\frac{3\ln\left(\frac{1+\omega_I^2\tau_m^2}{\left(\frac{\tau_m}{\tau_S}\right)^2+\omega_I^2\tau_m^2}\right) + 7\ln\left(\frac{1+\omega_S^2\tau_m^2}{\left(\frac{\tau_m}{\tau_S}\right)^2+\omega_S^2\tau_m^2}\right)}{4\ln\left(\left(\frac{\tau_S}{\tau_m}\right)^2\right) + 3\ln\left(\frac{1+\omega_I^2\tau_m^2}{\left(\frac{\tau_m}{\tau_S}\right)^2+\omega_I^2\tau_m^2}\right) + 13\ln\left(\frac{1+\omega_S^2\tau_m^2}{\left(\frac{\tau_m}{\tau_S}\right)^2+\omega_S^2\tau_m^2}\right)} \right) \tag{2}$$

where ω_I is the NMR frequency and ω_S is the paramagnetic electron resonance frequency ($\omega_S = 689\omega_I$). The theory is further explained in a companion paper [23].

3. Unilateral NMR instrumentation development

A one-sided portable magnet has been developed [2] with a polarisation field, B_0, of constant magnitude in a plane at a fixed distance above the device and with a gradient, G, in the field strength orthogonal to this plane. The magnetic field gradient is required to provide spatial resolution in the NMR measurement. The system also requires a radio frequency (RF) sensor designed such that the RF excitation field, B_1, is (ideally) everywhere orthogonal to the polarisation field. In the field gradient the thickness of the measured volume-slice is inversely proportional to the length of the applied RF excitation pulse and to the gradient strength.

The origin of the magnet design can be found in the primary of a permanent magnet linear eddy-current brake [24]. It is based on an infinite periodic array of individual magnetic blocks of thickness d and magnetisation, M_y, arranged to lie along the z-axis with the orientation of magnetisation alternating, as in Fig. 1A. The array period is $\lambda = 2\pi/\alpha$. The block magnetisation is expanded in a Fourier quarter series, viz:

$$M_y(z) = \sum_{m=1,3}^{\infty} M_{y,m}\cos(m\alpha z) \tag{3}$$

where

$$M_{y,m} = M_0\frac{4}{m\pi}\sin(m(\pi-\theta)/2) \tag{4}$$

and θ/α is the block spacing. For ideal neodymium iron boron (NdFeB), the magnetisation approximates to $M_0 = B_{\text{rem}}/\mu_0$, where the remanence B_{rem} is typically 1.2 to 1.4 tesla.

The condition that $|B_0|$ is constant in a plane above the magnet can only be met with a single Fourier harmonic, so the infinite array of blocks is modified to ensure that the $m = 1$ fundamental harmonic dominates. This is achieved by setting the mark-space-ratio to 2 : 1 ($\theta = \pi/6$): the 3rd harmonic reduces to zero while for $\alpha y \gg 1$ the other harmonics become negligible.

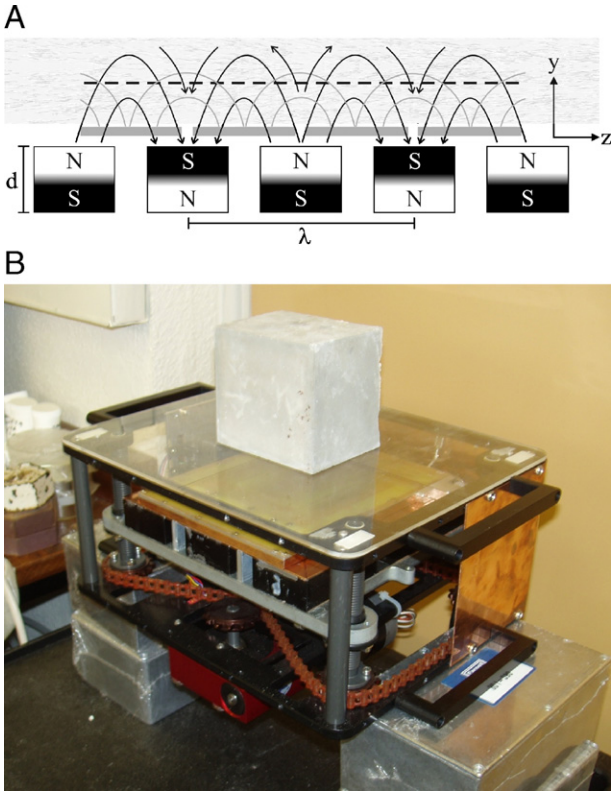

Fig. 1. (A) Alternating magnets (N/S) provide a plane (dotted line) of magnetic field of constant magnitude within the sample region (shaded) from which the NMR signal originates. The sensor coils (grey bars) are situated immediately above the magnets. The magnetic field lines (arrows) are always orthogonal to the RF field lines (grey lines). (B) The constructed magnet. Here three magnetic blocks are visible mounted on a motorised platform that can be moved relative to the sample. The RF sensor coil is on top of the magnet, with a cement block sample above the frame.

Hence the field profile can be approximated, for thin blocks ($\alpha d \ll 1$), by:

$$B_0 = \frac{1}{2}\mu_0 \alpha d M_{y,1} \exp(-\alpha y)(\cos(\alpha z)j + \sin(\alpha z)k) \quad (5)$$

where $M_{y,1} \approx (2\sqrt{3}/\pi)M_y$. For thin blocks, the presence of a steel back-plate on the blocks increases the field strength by a factor two. However for the relatively thick blocks used the effect is not so pronounced.

A similar argument can be used to design the surface RF sensor from current windings. If these are spatially offset from the magnetic blocks by $\lambda/4$, then the condition that the two fields are orthogonal is automatically met (Fig. 1A).

Practically it is not possible to manufacture an infinite magnet array: the array must necessarily be truncated. In our implementation the magnet array is truncated to three elements and the RF sensor to just two. Notwithstanding, it is possible to make a magnet that performs well over a significant plane orthogonal to the surface. Finite element modelling was used to refine the design so as to alleviate the end truncation effects. The finite length implementations lead to a correction where the central block is slightly narrower and the outer two blocks slightly wider than in the ideal design. The magnet has been constructed from blocks of NdFeB. Fig. 1B shows the magnet as built. The flat field plane produced corresponds to ^{1}H NMR resonant frequency of 3.2 MHz at a distance of 50 mm from the magnet surface and extends over a plane some $130 \times 100\,mm^2$. Here the field gradient is approximately $2.9\,Tm^{-1}$ in a direction perpendicular to the surface of the magnet. The probe is mounted across the three magnet blocks. Its more limited size ensures that most of the detected signal comes from the primary slice rather than peripheral regions at different depths. However, due to the curvature in $|B_0|$, approximately 16% of the measured signal still originates from sample outside this horizontal slice. The whole assembly (magnet and probe) is mounted in a frame and can be raised and lowered by a stepper motor relative to the frame so that the position (depth) of the excited slice within the external sample can be varied.

4. Experimental

Proton NMR T_1–T_2 two-dimensional relaxation correlation measurements were performed on samples of Ordinary Portland Cement (OPC) and white cement from two different manufacturers, referred to as white cements 1 and 2. Measurements were recorded using proton frequencies of 20 MHz (homogeneous bench top magnet). White cement 2 was also measured at 400 and 2 MHz using homogenous magnets. In all cases the measurements lasted approximately 5 h. The cement pastes were mixed in a water-to-cement (w/c) ratio of 0.4. All three of the homogeneous magnets (2, 20, and 400 MHz) can accommodate cylindrical samples 8 mm in diameter and 20 mm in length, cured in standard NMR tubes. Between measurements the samples were stored under water. Both white cement samples were also measured using the unilateral NMR magnet at 3.2 MHz. The single-sided magnet allows for much larger samples — in this case cubes of cement $100 \times 100 \times 100\,mm^3$. The samples for the unilateral magnet were cured in a high humidity environment and then sealed using a thin plastic wrapping. All the samples were first measured after 24 h of cure and were subsequently re-measured every 24 h for 7 days.

For the 20 MHz experiments, the pulse sequence consists of an inversion recovery immediately followed by a CPMG echo train containing n echoes, viz:

$$180°\text{–}t_1^{\text{encode}}\text{–}90°_x\text{–}\tau\text{–}[180°\text{–}\tau\text{–}(\text{echo})\text{–}\tau]_n \quad (6)$$

The two-dimensional data set comprises of the echo intensities (second dimension) recorded for each of a series of inversion recovery delays (first dimension). Both the inversion recovery delays and echo spacings were varied logarithmically so as to efficiently span the inversion recovery interval $t_1^{\text{encode}} = 0.1$ to 1000 ms and echo times from $2\tau = 0.068$ to 1680 ms. The pulse lengths used were 2.3 μs (corresponding to a 90° pulse) and 4.7 μs (corresponding to a 180° pulse).

The 2 and 400 MHz experiments utilised the same pulse sequence, with t_1^{encode} spanning the same time increments. However, the echo spacings had to be varied depending on the limitations of the system used. For the 2 MHz system the echo spacing (2τ) was constant at 200 μs. The pulse lengths used were 1.3 μs (90°) and 2.4 μs (180°). For the 400 MHz magnet the

echo spacing varied logarithmically to span the echo times from $2\tau=0.088$ to 2296 ms. The pulse lengths used were 18 μs (90°) and 37 μs (180°). For the measurements conducted in homogeneous magnetic fields the maximum echo intensities were used to create the T_2 relaxation decay curves.

For the one-sided magnet, the T_1 procedure was varied to saturation recovery and quadrature echoes were recorded so as to accommodate the strong field gradient:

$$90°-t_1^{\text{encode}}-90°_x-\tau-[90°_y-\tau-(\text{echo})-\tau]_n. \quad (7)$$

These changes make all the RF pulses of equal length ensuring that they excite a slice of approximately constant thickness [25]. The pulse length was 18 μs. It selected a slice approximately 0.5 mm thick about 10 mm below the surface of the sample. The echo spacing (2τ) was maintained constant at 0.3 ms; the t_1^{encode} intervals spanned the same logarithmic range as above. In these inhomogeneous field measurements the spin-echoes were integrated. To a good approximation the integral yields the echo intensity at the slice centre corresponding to the on-resonance position. The disadvantage of this sequence is that the resultant relaxation decay curves contain contributions from both T_1 and T_2 decays.

All the measurements were repeated at least once on repeat samples, often more times, and the results reported here were consistently observed.

5. Results

Fig. 2 (left column) shows a time series of T_1–T_2 correlation spectra for the white cement 1. These plots have been discussed previously in detail [6], so we only present a summary of the results here. The diagonal projection is a pore size distribution with the smallest (gel) pores lower-left, followed by capillary pores progressing to the upper right, with bulk water top-right. In each graph there are a series of discrete features parallel to the diagonal which represent water in different porosity environments. On day 1 there are two such peaks associated with gel and early stage capillary pores. The third peak, away from the diagonal is discussed below. By day 3 the diagonal peaks have become broadened and less distinct. The off-diagonal peak is still clearly visible. By day 7 two further features have evolved parallel to the diagonal associated with larger capillary pores. A final peak, top-right, is almost certainly residual surface water and water in larger micro-cracks. It can clearly be seen that these discrete diagonal features have a T_1/T_2 ratio of approximately 4, independent of pore size. Using Eq. (2) with the experimental NMR frequency of 20 MHz, a correlation time for diffusion of temporarily adsorbed molecules on the pore surfaces, τ_m, of 1.3 ns [26], and an estimate of the pore surface residency time, τ_s of 18.5 μs (consistent with field cycling results [23]) gives $T_1/T_2=4.0$, as observed.

The off-diagonal peak links the primary gel and capillary volumes. It is the first direct evidence of chemical exchange of hydrogen (water) between cement gel and capillary porosity. The intensity and position of the peak relates to the gel-capillary water exchange rate at the nano-scale. Although the equations

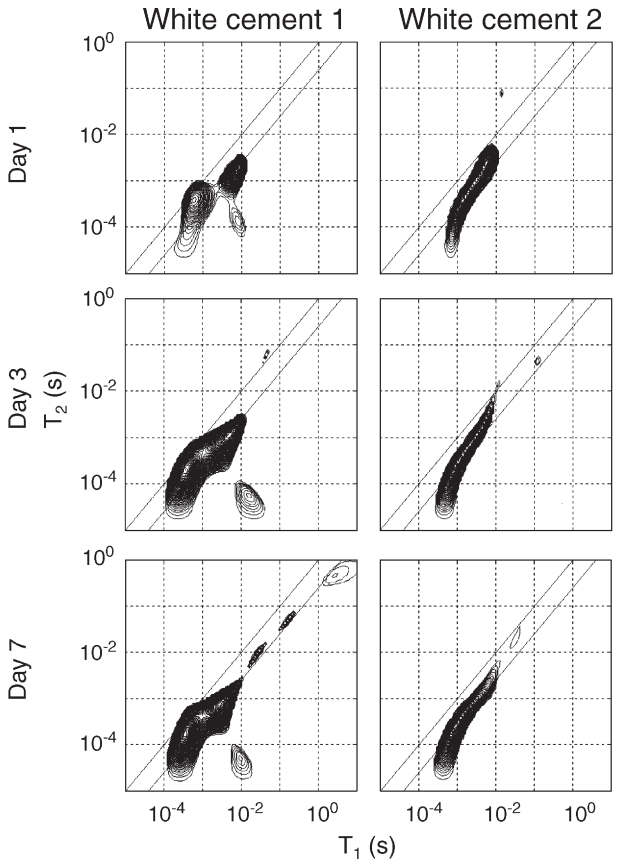

Fig. 2. T_1–T_2 two-dimensional relaxation correlation spectra of cement samples measured over 7 days using a 20 MHz (proton) bench top spectrometer: (left) white cement 1 and (right) white cement 2. In each plot a series of discrete features lie close to the quarter diagonal: $T_1=4T_2$ (lower solid line). There is also a single off-diagonal peak indicative of gel-capillary exchange in white cement 1.

describing the intensity of cross-relaxation peaks are known [6], a full analysis remains to be carried out. The asymmetry in the spectrum is understood theoretically insomuch as $T_1 \geq T_2$ is always true.

Fig. 2 (right column) shows the equivalent T_1–T_2 correlation spectra for the white cement 2. The difference between the two samples is immediately apparent: white cement 2 exhibits a continuous distribution of pore sizes parallel to the diagonal. This single feature remains almost unchanged throughout the course of the 7 day experiment. A small peak at long T_1 and T_2 times is just visible in all three plots and this is probably due to the formation of some larger pores. As with white cement 1, Fig. 2 (left column), the single feature in the white cement 2 plots exhibits a T_1/T_2 ratio of approximately 4. This indicates that the pore surface diffusivity and residency correlation times (τ_m and τ_s respectively) are very similar, suggesting comparable intra-pore water dynamics. Significantly there is no exchange peak visible in any of the white cement 2 spectra. In an attempt to explain these differences, both the particle size distribution of the raw powder and the phase composition of the hydrated material have been measured for both cements [27]. X-ray diffraction (XRD) analysis suggests that the phase composition of the two materials is the same within experimental error. The initial particle size distribution of the two cements is however

different with the white cement 2 being noticeably finer (having a mean particle diameter of 8 μm compared to 12 μm for white cement 1). The different particle sizes could conceivably change the microstructure of the hydrated material and underlie the NMR differences observed. However, different pre-hydration aging of the materials cannot be ruled out.

As a contrast to the two white cement samples, an OPC paste was also studied. The results can be seen in Fig. 3. Initially (day 1) a single extended feature is present along the half-diagonal. Below this feature is an off-diagonal peak suggesting that chemical exchange between pores of two distinct sizes (gel and capillary) is occurring. These features are observed in spite of the significantly greater Fe^{3+} ion content of OPC compared to white cement. By day 3 the single large feature visible on day 1 has resolved into a bi-modal distribution but the exchange peak is no longer visible. Also, two further distinct peaks have emerged at longer T_1 and T_2 relaxation times. These continue through to day 7. The primary peaks exhibit a T_1/T_2 ratio of approximately 2, compared to 4 in the white cements. Elsewhere [23] it is suggested that τ_m is remarkably constant at approximately 1.0 ns over a range of cement materials. Using this value and the ratio $T_1/T_2=2$ at 20 MHz suggests $\tau_s=0.1$ μs. This is a shorter residency time than experienced in the white cement, implying that the water molecules spend less time on the pore surface.

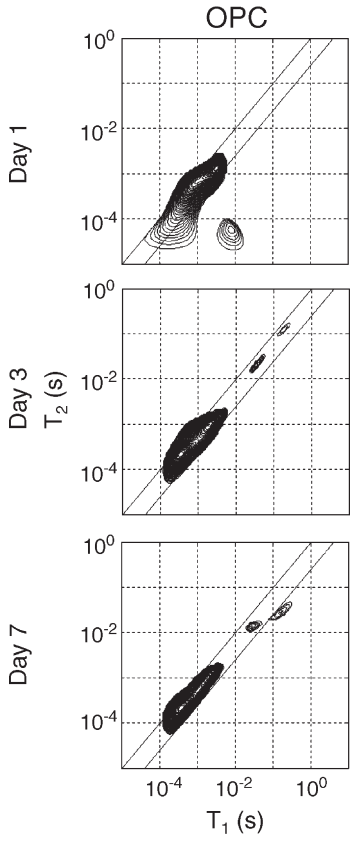

Fig. 3. T_1–T_2 two-dimensional relaxation correlation spectra from an OPC sample cured over 7 days using a 20 MHz bench top spectrometer. For the main peaks in this sample, $T_1=2T_2$, compared to $T_1=4T_2$ in white cement (lower solid line). There is an off-diagonal exchange peak on day 1.

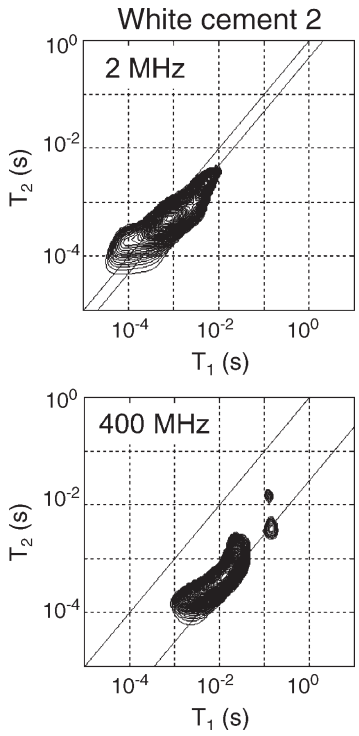

Fig. 4. T_1–T_2 two-dimensional relaxation correlation spectrum for white cement 2 measured at (top) 2 MHz and (bottom) 400 MHz, recorded after 3 days of cure. As indicated by the lower solid lines, the T_1/T_2 ratios are approximately 2 and 35, respectively.

In order to verify the frequency dependence of the T_1/T_2 ratio as defined in Eq. (2), white cement 2 was additionally measured at proton resonant frequencies of 2 and 400 MHz. The single main peak characteristic of this cement (see Fig. 2 right column) lies parallel to the $T_1=T_2$ line and it is assumed that the ratio of T_1/T_2 defined by this feature is representative

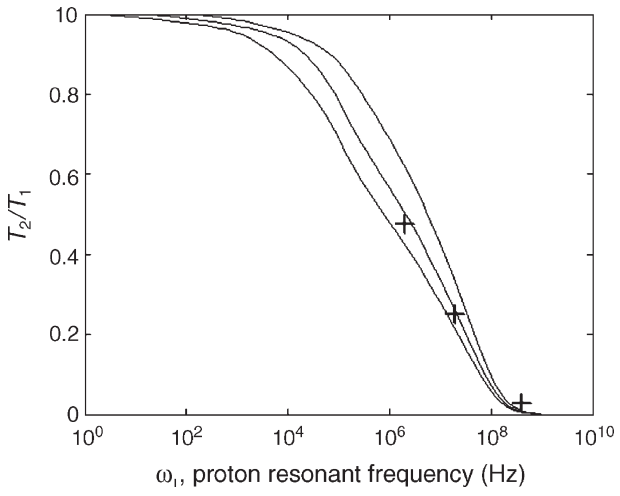

Fig. 5. Frequency dependence of T_2/T_1 as a function of proton resonant frequency. The solid lines have been generated using Eq. (2) with $\tau_m=1.3$ ns. The three lines correspond to τ_s values equal to $10^2\times\tau_m$ (lower), $10^3\times\tau_m$ (middle) and $10^4\times\tau_m$ (upper). The experimental estimates of T_2/T_1 obtained for white cement 2 at three days cure (from Figs. 2 and 4) are shown on the plot (+) to compare with the theoretical model.

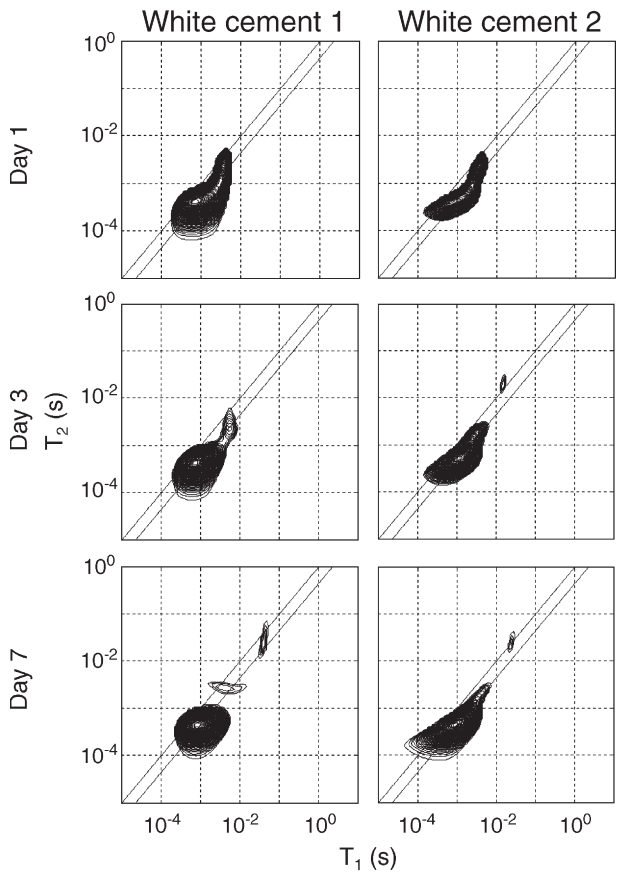

Fig. 6. T_1–T_2 two-dimensional relaxation correlation spectra of white cement samples measured using a 3.2 MHz (proton) portable unilateral magnet. The signal originates from a slice approximately 0.5 mm thick some 10 mm below the surface of the sample. The plots are broadly similar to those measured under ideal conditions at 20 MHz, except that no exchange peak is observed. In all the graphs the principle features lie close to the line $T_1/T_2=2.25$ as predicted by Eq. (2).

of the two-dimensional diffusion of water on the pore surface. This single characteristic feature was observed at both 2 and 400 MHz (see Fig. 4). On both plots, a line was placed through the centre of the main elongated feature, parallel to the $T_1=T_2$ line. In this way the T_1/T_2 ratios were estimated at 2 MHz as 2.1 ± 0.2 and at 400 MHz as 35 ± 5. These values were inverted to provide a T_2/T_1 ratio and compared to the theoretical model in Eq. (2), see Fig. 5. The three T_2/T_1 ratios provide a close fit to the model when using correlation times $\tau_m=1.3$ ns and $\tau_s=13$ μs. The largest deviation from the model occurs at 400 MHz where theoretically $T_1/T_2\sim138$.

To demonstrate the capabilities of the one-sided magnet, large blocks of both cements were measured to provide a T_1–T_2 relaxation correlation from a slice in a large sample. Preliminary results can be seen in Fig. 6. From Eq. (2), at 3.2 MHz, the calculated ratio $T_1/T_2=2.25$, a smaller value than at 20 MHz and close to that observed experimentally. However, the spectra are relatively featureless and in particular we see neither discrete diagonal features nor off-diagonal exchange peaks in white cement 1. One reason may be that these samples were cured sealed and may therefore lack features associated with more mobile water and longer relaxation times. Equally it may be because the signal-to-noise ratio is lower, there are fewer data points, and the minimum observable echo (T_2) time is 300 μs compared to 68 μs in the bench top measurement.

6. Conclusions

Previously we demonstrated the wealth of information available from two-dimensional relaxation correlation studies of a white Portland cement compared with more conventional one-dimensional analyses, highlighting the clarity with which distinct pore size distribution features can be observed [6]. Here we have extended this technique to look at two other cement pastes: a second white Portland cement from a different manufacturer and OPC. Significant differences have been observed between the three. With further study this technique may lead to a sensitive and non-destructive characterisation method for pore water interactions in cements. We have also verified the frequency dependence of the theoretical model for the ratio of T_1/T_2 used to interpret the data.

We have also shown that it is possible to make T_1–T_2 two-dimensional relaxation correlation experiment measurements in cement blocks using a portable one-sided NMR magnet system. Although the preliminary data is not yet as rich in features as the laboratory data it agrees in broad outline especially insofar as the T_1/T_2 ratio is as expected.

With time, and as methodology develops, we believe that it will be possible to gain as much information from sub-surface slices in situ as it is possible to gain under ideal laboratory conditions from test samples. However, at this stage, both the two-dimensional correlation relaxometry and in situ technology remain in their infancy.

Acknowledgements

We thank Y.-Q. Song of Schlumberger-Doll Research for the use of a copy of his two-dimensional Fast Laplace Inversion (FLI) software. We thank K. Scrivener for the results of phase analysis and particle size distribution for the white cements. LM thanks The NANOCEM Consortium and JM thanks The Royal Society, for financial support.

References

[1] Y.-Q. Song, L. Venkataramanan, M.D. Hürlimann, M. Flaum, P. Frulla, C. Straley, T_1–T_2 correlation spectra obtained using a fast two-dimensional Laplace inversion, J. Magn. Reson. 154 (2002) 261–268.
[2] P.J. McDonald, P.S. Aptaker, GB pat. application no. GB0426957.7 (2004).
[3] P.T. Callaghan, I. Furo, Diffusion–diffusion correlation and exchange as a signature for local order and dynamics, J. Chem. Phys. 120 (2004) 4032.
[4] L. Venkataramanan, Y.-Q. Song, M.D. Hürlimann, Solving Fredholm integrals of the first kind with tensor product structure in 2 and 2.5 dimensions, IEEE Trans. Signal Process. 50 (5) (2002) 1017–1026.
[5] B.P. Hills, S. Benamira, N. Marigheto, K. Wright, T_1–T_2 correlation analysis of complex foods, Appl. Magn. Reson. 26 (2004) 543.

[6] P.J. McDonald, J.-P. Korb, J. Mitchell, L. Monteilhet, Surface relaxation and chemical exchange in hydrating cement pastes: a two-dimensional NMR relaxation study, Phys. Rev., E 72 (2005) 011409.
[7] M.D. Hürlimann, L. Venkataramanan, Quantitative measurement of two-dimensional distribution functions of diffusion and relaxation in grossly inhomogeneous fields, J. Magn. Reson. 157 (2002) 31.
[8] B. Sun, K.-J. Dunn, A global inversion method for multi-dimensional NMR logging, J. Magn. Reson. 172 (2005) 152.
[9] A.J. Bohris, U. Goerke, P.J. McDonald, M. Mulheron, B. Newling, B.L. Page, A broad line NMR and MRI study of water and water transport in Portland cement pastes, Magn. Reson. Imaging 16 (5/6) (1998) 455–461.
[10] G. Eidmann, R. Savelsberg, P. Blümler, B. Blümich, The NMR MOUSE, a mobile universal surface explorer, J. Magn. Reson., Ser. A 122 (1996) 104–109.
[11] J.A. Jackson, R.K. Cooper, L.J. Burnett, J.F. Harmon, Remote NMR well logging, Geophysics 46 (1981) 415.
[12] R.L. Kleinberg, A. Sezginer, D.D. Griffin, M. Fukuhara, Novel NMR apparatus for investigating an external sample, J. Magn. Reson. 97 (3) (1992) 466–485.
[13] E. Fukushima, J.A. Jackson, Unilateral Magnet having a Remote Uniform Field Region for Nuclear Magnetic Resonance, US Pat 6,489,872 (1999).
[14] P.T. Callaghan, NMR Apparatus, New Zealand pat. application no. 520114.
[15] A.E. Marble, I.V. Mastikhin, B.G. Colpitts, B.J. Balcom, An analytical methodology for magnetic field control in unilateral NMR, J. Magn. Reson. 174 (1) (2005) 78–87.
[16] K.R. Brownstein, C.E. Tarr, Importance of classical diffusion in NMR studies of water in biological cells, Phys. Rev., A 19 (6) (1979) 2446–2453.
[17] W.P. Halperin, F. D'Orazio, S. Bhattacharja, J.C. Tarczon, Magnetic resonance relaxation analysis of porous media, in: J. Klafter, J.M. Drake (Eds.), Molecular Dynamics in Restricted Geometries, Wiley, 1989, pp. 311–350.
[18] W.E. Kenyon, Nuclear-magnetic-resonance as a petrophysical measurement, Nucl. Geophys. 6 (2) (1992) 153–171.
[19] R.L. Kleinberg, Well logging, in: D.M. Grant, R.K. Harris (Eds.), Encyclopedia of NMR, J. Wiley & Sons, 1996, p. 4960.
[20] W.P. Halperin, J.-Y. Jehng, Y.-Q. Song, Application of spin–spin relaxation to measurement of surface area and pore size distributions in a hydrating cement paste, Magn. Reson. Imaging 12 (2) (1994).
[21] J. Greener, H. Peemoeller, C. Choi, R. Holly, E.J. Reardon, C.M. Hansson, M.M. Pintar, Monitoring of hydration of white cement paste with proton NMR spin–spin relaxation, J. Am. Ceram. Soc. 83 (3) (2000) 623–627.
[22] S. Godefroy, J.-P. Korb, M. Fleury, R.G. Bryant, Surface nuclear magnetic relaxation and dynamics of water and oil in macroporous media, Phys. Rev., E 64 (2001) 021605.
[23] J.-P. Korb, L. Monteilhet, P.J. McDonald, J. Mitchell, Microstructure and texture of hydrating cement-based materials: a proton field-cycling relaxometry approach, Cement Concrete Res. 37 (2007) 295–302 (this volume).
[24] J.D. Edwards, B.V. Jayawant, W.R.C. Dawson, D.T. Wright, Permanent-magnet linear Eddy-current brake with a non-magnetic reaction plate, IEE Proc., Electr. Power Appl. 146 (6) (1999) 627–631.
[25] M.D. Hürlimann, Carr–Purcell sequences with composite pulses, J. Magn. Reson. 152 (1) (2001) 109–123.
[26] F. Barberon, J.-P. Korb, D. Petit, V. Morin, E. Bermejo, Probing the surface area of a cement-based material by nuclear magnetic relaxation dispersion, Phys. Rev. Lett. 90 (11) (2003) 116103.
[27] Personal Communications with K. Scrivener, EPFL, Lausanne, Switzerland. 2005.